Inorganic Chemistry

ARTICLE

pubs.acs.org/IC

Reactive Facets Covered Mosaic Spheres of Anatase TiO_2 and Related Pseudo-Isotropic Effect

Guolei Xiang, Tianyang Li, and Xun Wang*

Department of Chemistry, Tsinghua University, Beijing, 100084, P. R. China

Supporting Information

ABSTRACT: Pseudo-isotropic mosaic spheres of anatase almost completely covered with reactive (001) facets are prepared via a one-pot reaction. The growth process is mediated by an appropriate amount of NaF under hydrothermal conditions. Due to the large exposure ratio of identical (001) facets, the product can serve as an ideal model to investigate certain crystalline plane effects owing to their pseudo-isotropic properties, such as texture effects. Intensified X-ray diffraction results are presented to show such effects induced by morphology.

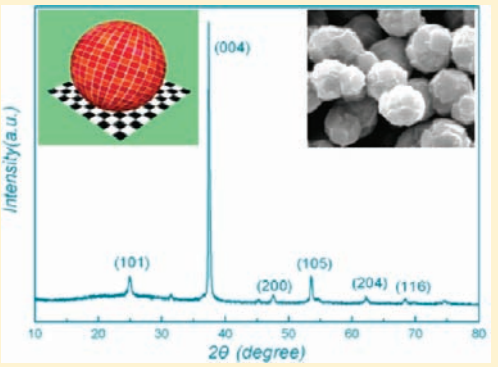

INTRODUCTION

Insights into many basic processes related with surface reactions, like heterogeneous catalysis, photocatalysis, dye-sensitized solar cells, and so on, rely on recognizing the surface structures and chemical and physical processes therein.[1,2] Concerning these basic issues of surface chemistry and physics, single crystals exposing single-crystalline facets are usually employed to learn the mechanisms of various surface changes.[3,4] Among those studies, the reactive facets of inorganic minerals have been followed with interest due to the importance for both fundamental research and practical applications.[5] However, it is quite challenging to selectively expose these high-energy facets because they usually diminish quickly during growing up to minimize the total surface energy. As for anatase, an extensively studied polymorph of TiO_2 in the area of energy conversion and environment improvement, the average surface energy of {001} facets (0.90 J m^{-2}) is much higher than that of thermodynamically stable {101} (0.44 J m^{-2}).[6] Key progress was made by using hydrofluoric acid as the morphology-controlling agent on the basis of first-principles calculation results; thus, anatase single crystals exposing 47% (001) facets were successfully synthesized.[7] These reactive facets abundant anatase materials are thought to exhibit higher photocatalytic reactivities than normal titania,[8−11] so it is of value to maximize the exposure ratio of these reactive facets.

To fully utilize the functions of a specific crystalline plane, many efforts have been made to prepare nanocrystals of different regular shapes. In addition, there are currently two major routes to construct ideal geometry models composed of maximum identical facets. For crystals of a highly symmetrical cubic system, isotropic structures can be realized in the forms of regular polyhedra, such as a cube for {001} facets and an octahedron for {111}.[12,13] In the case of anatase, a less symmetrical tetragonal crystal, increasing the exposure ratio of identical reactive {001} facets, should be alternatively realized by means of decreasing the thickness along the *c* axis to form nanosheets as thin as possible.[8,9,14] The {001} exposure ratio of anatase has been increased from 47% to 64% and 89% in this way via modified solvothermal and hydrothermal reactions. Herein, we present another approach to maximize the exposure ratio of reactive anatase (001) facets by forming pseudo-isotropic mosaic spheres as shown by the model in Figure 1a. Because the surfaces are composed of anatase sheets, this structure is almost completely covered with the reactive {001} facets. The materials were prepared via a one-pot hydrothermal reaction. In a typical preparation procedure, 0.5 mL of $TiCl_3$ aqueous solution (∼15%) and 5 mmol of NaF were dissolved in 30 mL of deionized water in a Teflon-lined autoclave. After being hydrothermally treated at 200 °C for 6 h, microspheres of anatase were obtained and washed with water.

EXPERIMENTAL DETAILS

Chemicals. Titanium(III) chloride ($TiCl_3$) solution (15−20%) was purchased from Sinopharm Chemical Reagent Co., Ltd. (Shanghai, China). Sodium fluoride (NaF) was from Beijing Chemical Reagent Co. The water used in all experiments was deionized water. All reagents were used as received without further purification.

Synthesis of Anatase Mosaic Spheres at 200 °C. In a typical synthetic procedure, 0.5 mL of $TiCl_3$ aqueous solution and a certain

Received: March 17, 2011
Published: June 06, 2011

   dx.doi.org/10.1021/ic200553t | *Inorg. Chem.* 2011, 50, 6237–6242

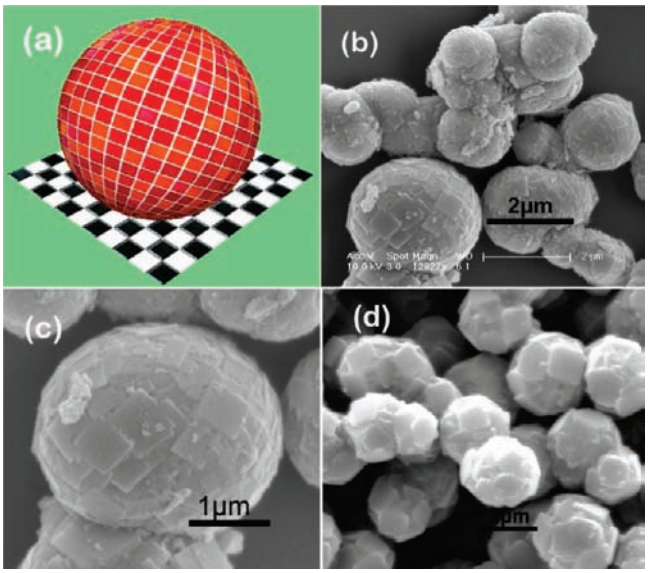

Figure 1. (a) Model of a mosaic sphere covered with identical building blocks. (b and c) SEM images of anatase mosaic spheres covered with (001) facets prepared at 200 °C. (d) SEM image of the spheres prepared at 150 °C using 5 mmol of NaF.

amount of NaF (from 0 to 9 mmol) were mixed with water in a 40 mL Teflon-lined stainless steel autoclave. The total volumes of reaction solutions were 32 mL. After being sealed, the reactants were hydrothermally treated at 200 °C for 6 h; mosaic spheres of anatase were obtained and washed with water for several times. To acquire the evolution details, the reactions were conducted at different concentrations of NaF by varying the reaction time. The reactions can be also conducted at lower temperature, such as 150, 120, and 95 °C.

Photocatalytic Test. Photocatalytic degradation of Methyl Orange (MO) under ultraviolet light was used to evaluate the reactivity of the mosaic spheres. A 0.1 g amount of sample was dispersed in 150 mL of deionized water by ultrasonication for 10 min and then mixed with MO (3 mL, 1 mmol/L) in a reactor. Before irradiation, the solution was stirred in the dark for 30 min to ensure equilibrium of the working solution. The reaction was irradiated by a 300 W xenon lamp, and the decreasing concentration of MO was reflected by monitoring the absorbency at 465 nm. Before measuring the absorbency, the samples were centrifugated to remove the catalysts.

Characterization. Size and morphology of the mosaic spheres were determined on a Tecnai TF20 S-Twin high-resolution transmission electron microscope (HRTEM) at 200 kV and a JEOL JSM-6700F scanning electron microscope (SEM). The samples were prepared by dropping an ethanol dispersion of samples onto Si substrate or carbon-coated copper grids by immediately evaporating the solvent. The X-ray diffraction (XRD) patterns of samples were recorded on a Rigaku D/max-2400 diffractometer operated at 40 kV voltage and a 200 mA current with Cu Kα radiation (λ = 1.5418 Å).

■ RESULTS AND DISCUSSION

Morphological information characterized by scanning electron microscopy (SEM, Figures 1 and S1, Supporting Information) shows that the products are micrometer-sized spheres. However, they are quite different from other colloidal spheres which are usually amorphous or composed of aggregated smaller nanoparticles.[15,16] These TiO_2 microspheres have a mosaic structure composed of sheets inlaid on the outside surfaces, with a size ranging from 1 to 2 μm. It can be seen that all these building

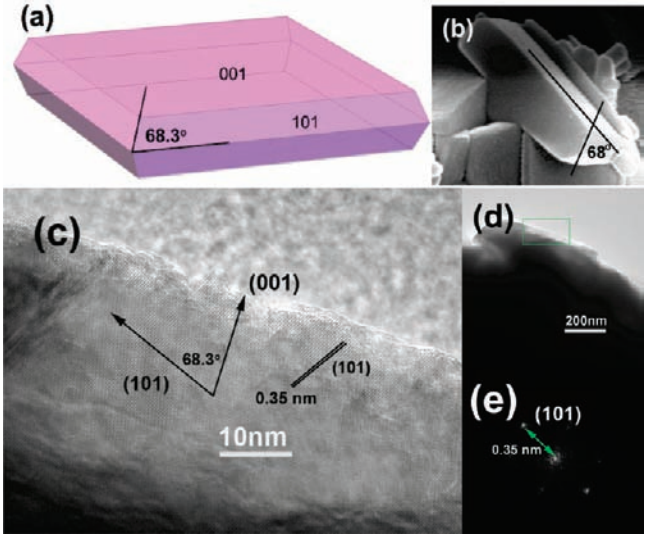

Figure 2. (a) Schematic model of a highly truncated tetragonal bipyramid exposing (001) and (101) facets, (b) measurement of the interfacial angle of a relatively isolated shell unit, (c) determining the exposing facet by analyzing lattice parameters of HRTEM image, (d) location of a surface building block for HRTEM analysis, and (e) corresponding Fourier transformation showing the spots of (101) facets.

blocks share a similar shape with the reactive anatase nanosheets prepared from HF involved systems, known as highly truncated tetragonal bipyramids. It is known that the facets and orientations in crystals have constant geometric configurations due to their intrinsic group symmetry, so it is a feasible way to index the exposed planes from the symmetry of their crystal morphologies. Measurement of interfacial angles of the shell units in SEM images can provide some information of the crystallographic structure. The geometrical parameters of relatively isolated shell sheets, which are prepared by increasing the amount of Ti precursors at 200 °C, are shown in Figure 2b, compared with a schematic model (Figure 2a). The interfacial angles are determined to be around 68°, consistent with that between anatase (001) and (101) facets (Figure 2a). Thus, the outside surfaces of the spheres can be indexed to be (001) planes of anatase according to such shape symmetry.

In addition to the shape symmetry, analysis of lattice parameters in HRTEM images is a useful proof to determine the crystallographic orientation of nanocrystals. Unfortunately, due to their large micrometer sizes, it is difficult for electron beams to pass through these spheres, so it is hard to conduct selected area electron diffraction (SAED) or acquire the high-resolution transmission electron microscopy (HRTEM) images of well-oriented surface sheets. For that reason we conducted the HRTEM analysis on a sheet located at the surface edge. The results are shown in Figure 2c–e. It is the lateral image of a prominent sheet. Lattice spacing of the apparent fringes in the HRTEM image is determined to be 0.35 nm according to its Fourier transformation result (see Figure 2e), and it can be assigned to the (101) facet of anatase. Since the inherent angle between (101) and (001) facets is about 68.3°, the exposed surface planes can be well indexed to be (001) facet by analyzing the geometric parameter as displayed in Figure 2c. Therefore, on the basis of both geometrical parameters and lattice features, we can draw the conclusion that the surfaces of these mosaic spheres are covered with a very large percentage of reactive (001) anatase facets.

dx.doi.org/10.1021/ic200553t |*Inorg. Chem.* 2011, 50, 6237–6242

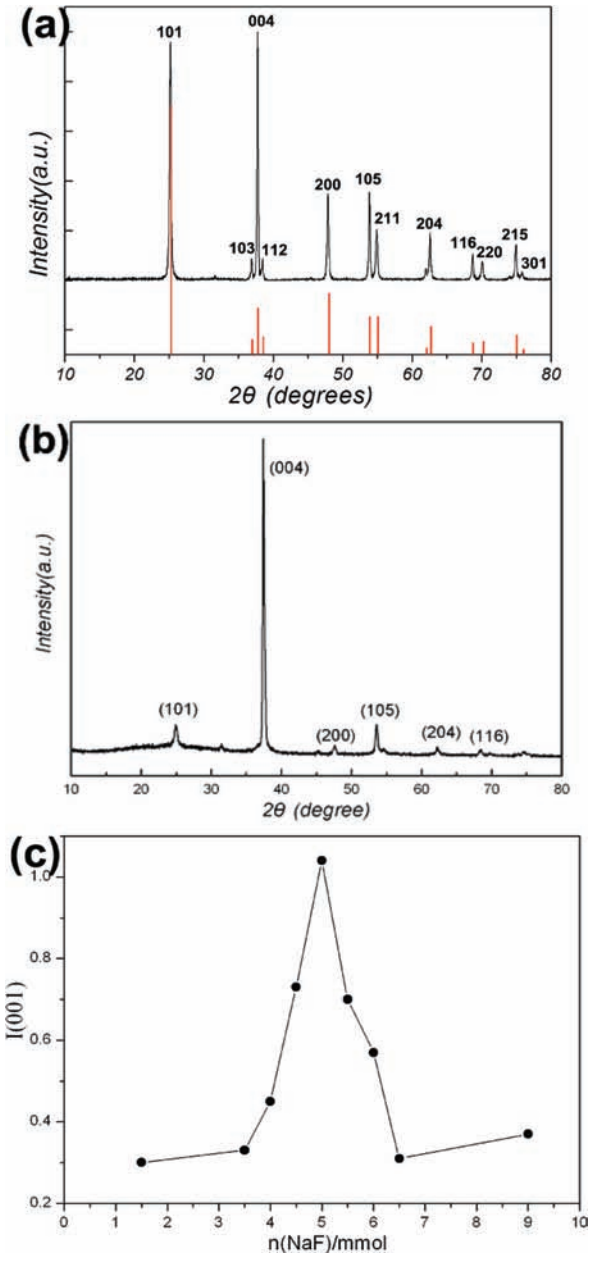

Figure 3. (a) XRD pattern of the anatase mosaic spheres prepared at 200 °C. (b) XRD pattern of anatase sample prepared at 150 °C. (c) Correlation of (004) diffractive intensities with the amount of NaF synthesized at 200 °C.

Crystals covered with specific facets can serve as ideal models to investigate the effects of different crystalline planes on catalysis, gas sensing, surface adsorption, etc.,[17,18] so well-shaped nanostructures are of great value to learn the issues. We found the present anatase mosaic spheres have an unusual pseudo-isotropic property toward X-ray diffraction (XRD). It is known that X-ray diffraction intensities have some relationship with the preferred orientation of crystalline grains besides their geometric structure factors. Facets with a larger exposure fraction usually diffract more intensively than those of random bulk materials. In materials science, such phenomena are referred to be texture effect, which originates from an oriented arrangement of crystallographic facets. Texture is an effect that is dependent on the

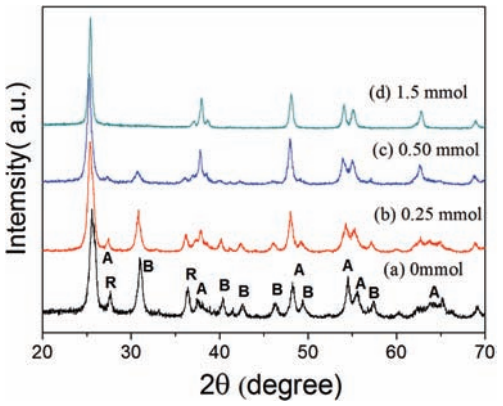

Figure 4. XRD patterns indicating the phase evolution results of TiO_2 by altering the amount of NaF.

degree of oriented arrangement; thus, it can be weak, moderate, or strong. X-ray diffraction is the mostly widely used technology to determine the texture effect of polycrystalline samples for the intensity of certain peaks can be increased many times due to their preferred orientations. As to the present mosaic spheres, which are covered with anatase sheets, the exposure ratio of (001) facets is increased by means of an outward mosaic arrangement, forming another type of texture effect that is different from conventional forms. It is an intrinsic texture effect by preferred orientation of (001) facets on the surface. This morphological feature enables a pseudo-isotropic property by their identical shell units. Figure 3a presents the XRD pattern of the (001) facets covered mosaic spheres prepared at 200 °C. This pattern can be well assigned to the anatase phase of TiO_2 (JCPDS 84-1285), but it is more noteworthy that the diffractive intensity of the (004) peak at 37.8° has been enhanced markedly compared with previously reported results of anatase single crystals exposing reactive facets.[7−9,19] This peak intensity has been increased from 0.18 to 1.04 with respect to the intensity of the characteristic (101) peak at 25.3° (I_{004}/I_{101}), so this means a larger diffractive opportunity for (004) than other facets. Particularly, the diffraction intensity can be even promoted. Figure 3b displays the diffraction result of a sample prepared at 150 °C by using an optimum amount of NaF (∼5 mmol). The peak intensity of reactive (004) facet is determined to be 15.87, nearly 2 orders of magnitude higher than the literature value. This stronger enhancement effect originates from the apparent isotropic structure of mosaic spheres, for their surfaces are almost completely covered with a single facet, as shown by the SEM image in Figure 1d.

Since the anatase mosaic spheres were prepared in the presence of NaF, to acquire insights into its roles, we further investigated the evolution processes by altering the amount of NaF at 200 °C. Figure 3c and Figure S2 and Table S1, Supporting Information, give the dependence of the relative diffractive intensity of the (001) peak upon the amount of NaF used in the reaction system, which is defined as I_{001}/I_{101} based on their actual diffraction intensities. It can be seen that there exists an optimal amount of NaF for maximizing the exposure fractions of the high-energy facet. The maximum intensity was achieved when 5 mmol of NaF was adopted. This correlation indicates that neither lower nor higher dosages of capping agents favor exposure of {001} facets. An appropriate F^- concentration is critical to get the strongest diffraction intensity. This trend was also found

dx.doi.org/10.1021/ic200553t |*Inorg. Chem.* 2011, 50, 6237–6242

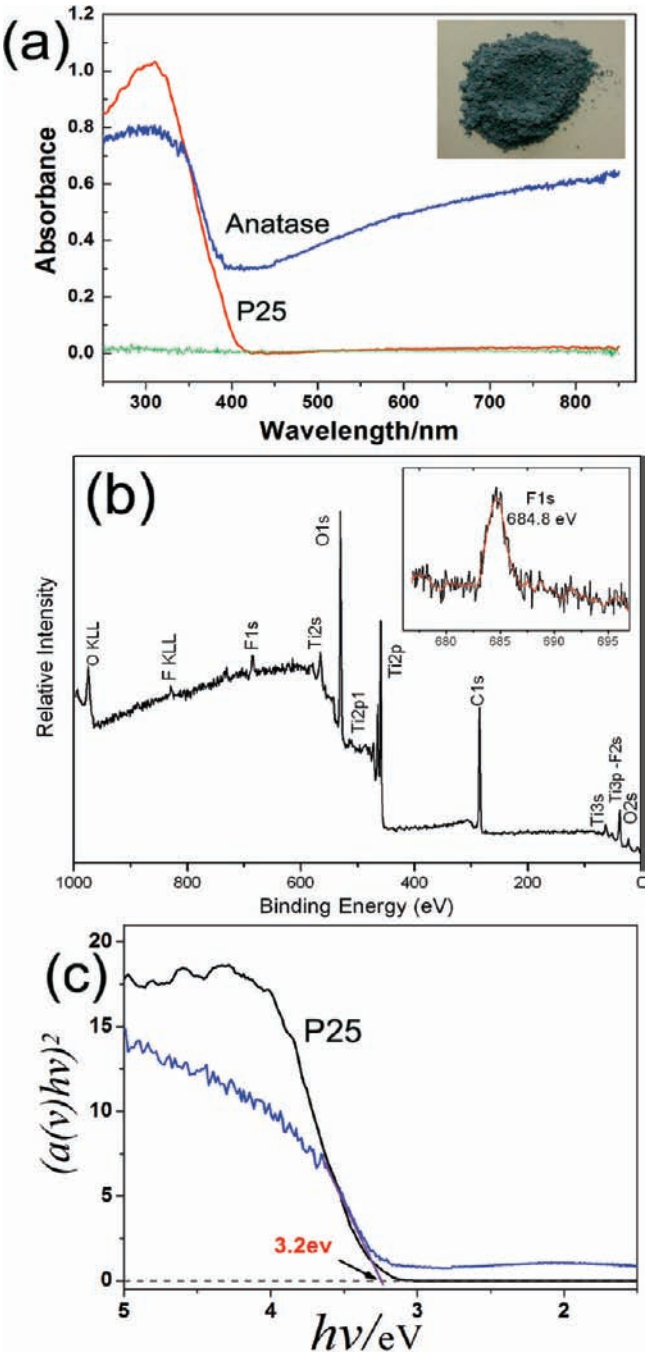

Figure 5. (a) UV−vis diffuse reflection spectroscopy of anatase microspheres. (Inset) Camera image of the sample. (b) XPS survey spectra of anatase mosaic spheres prepared at 200 °C. (Inset) High-resolution XPS spectra of the F1s peak. (c) Estimation of the band gap energy of mosaic spheres compared with P25.

when the reaction was conducted at lower temperature (Figure S3, Supporting Information). All optimum amounts of NaF are around 5 mmol. Besides the role as a shape-controlling agent, we found that NaF also served as a phase inducer. Phase evolution results characterized via XRD are shown in Figure 4 by changing the amounts of NaF. All of the three common phases, rutile, anatase, and brookite, appear in the product in the absence of NaF. In addition, brookite dominates in content while rutile exhibits the weakest intensities. Their relative ratio is sensitive to

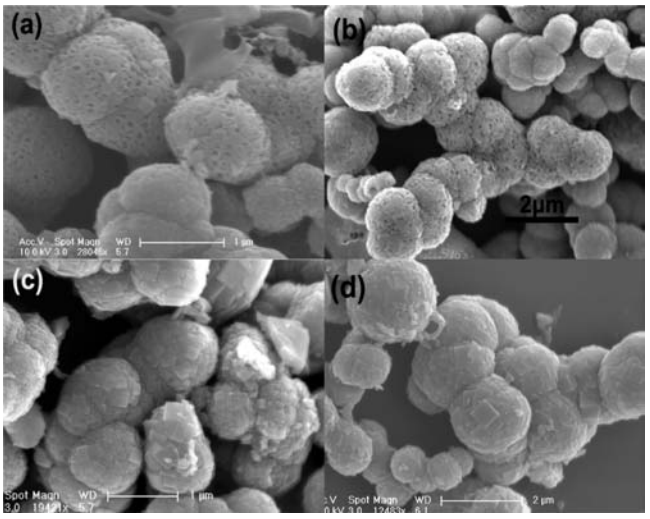

Figure 6. SEM images of evolutional processes at different reaction times: (a) 1, (b) 2, (c) 4, and (d) 6 h.

introduction of fluorine anions. When increasing its amount, brookite and rutile will gradually disappear from the final products and pure anatase phase rises in the presence of 1.5 mmol of NaF. Both the selectivity in anatase phase and its reactive facets originates from the strong coordination of fluorine anions with Ti cations as well as the surfaces of anatase. The color change of precursory solutions from purple to light green on adding NaF indicates an obvious transformation of Ti^{3+} from hydration to fluorine coordination.

The strong interaction between F and Ti is also reflected in the color of the final products apart from the above effects on phase formation and shape control. Figure 5a displays the UV−vis diffuse reflection spectroscopy result of mosaic sphere samples prepared at 200 °C. Compared with P25, a commercial titania product composed of anatase and rutile, the present sample has obvious absorption in the visible light region. This modified optical property can be further certified by the steelblue color as shown by the inset camera image. The element composition and chemical states are analyzed by the X-ray photoelectron spectrum (XPS, Figure 5b). It further proves that fluorine anions remain in the mosaic spheres, but the binding energy of F1s at 684.8 eV revealed by high-resolution XPS data indicates most fluorine ions are adsorbed species on the surfaces.[20] The result implies that this color feature may originate from surface defects by F adsorption. The UV−vis absorption spectrum of a semiconductor contains information on its band gap. For TiO_2, a direct band semiconductor, the variation in absorption coefficient ($\alpha(v)$) as a function of photon energy (hv) close to a band edge can be fitted to the following formula $[\alpha(v)hv]^2 = B(hv - E_g)$, where B is a constant and E_g is the band gap energy. The result is displayed in Figure 5c, showing that the bulk band gap is not changed in the presence of fluorine anions, which is about 3.2 eV. Thus, such enhanced adsorption in the visible light region comes from the surface defects by F coordination.

As the mosaic spheres are constructed by anatase nanosheets, to learn more details on the formation mechanism, the intermediate products at different reaction stages were investigated in terms of SEM. Figure 6 details the morphological evolution within a period of 6 h. It can be seen that most of the spheres are porous on the surfaces after 1 h. Their surfaces are covered by

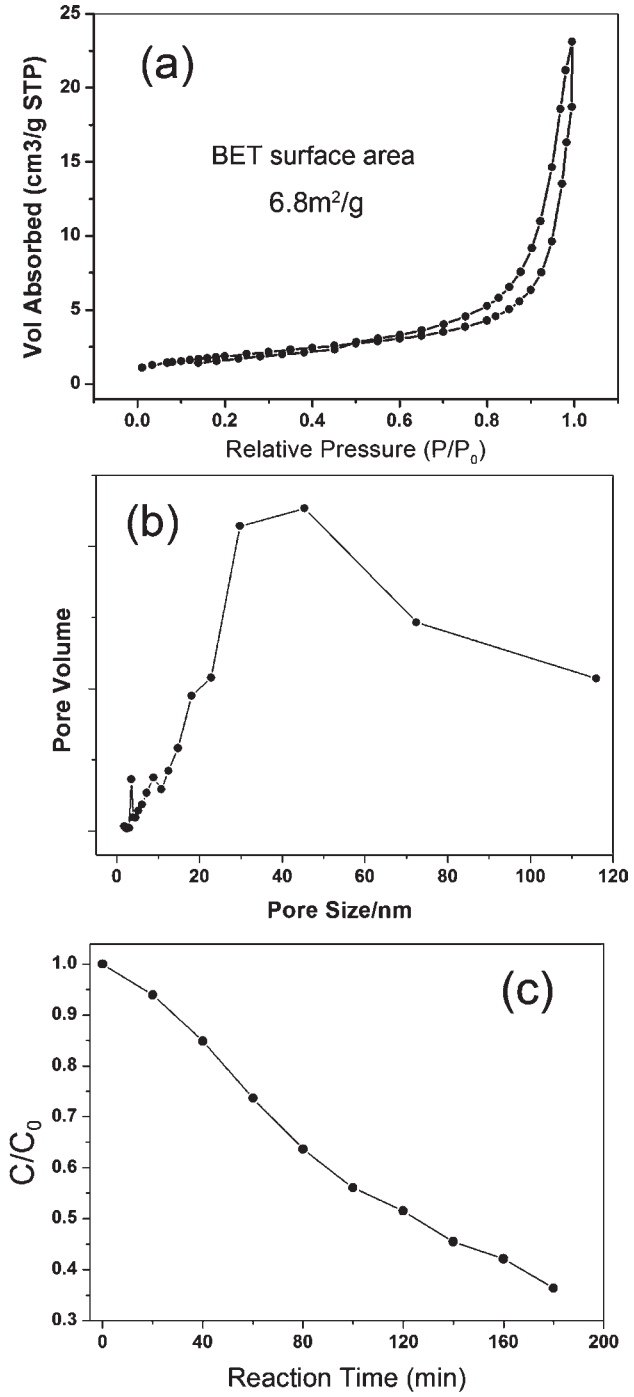

Figure 7. Nitrogen adsorption and desorption curve of the mosaic spheres (a), and corresponding pore size distribution result (b). (c) Photocatalytic degradation result of methyl orange by the spheres under ultraviolet irradiation.

particles and untypical nanosheets. Even more nanosheets have appeared after 2 h, with the decrease of the surface holes. It is noted that the inner part of the 2 h product is also composed of anatase sheets exposing (001) facets but looks looser than the final products. These porous surfaces will ultimately be replaced by nanosheets of several hundred nanometers after 4 h (Figure 6c). By further increasing the reaction time to 6 h, mosaic spheres almost completely covered with reactive facets become the major products. This evolution process shows that this pseudo-isotropic structure is established at the final stage via in situ growth on the surface of porous transition media. It is fluorine ions that undoubtedly induce formation of these reactive facets. On the other hand, we find that Na cation is also an important factor that promotes formation of such mosaic structure. Only random aggregates were obtained when replacing NaF by NH_4F, and the reactive (001) facets were also not perfectly developed as shown by Figure S4, Supporting Information, leaving a lot of holes on these surfaces. To further learn the internal structure and formation mechanism, we characterized the surface via N_2 adsorption and desorption (Figure 7a and 7b). The whole BET surface area is about 6.8 m^2/g, including both the outside surface and the hidden inner surface. The pore distribution result shows the pore sizes range from 20 to 80 nm, indicating the existence of an inner space between the stacked sheet units. As an important photocatalyst, we tested the performance of the mosaic spheres in degrading methyl orange under ultraviolet irradiation. The result is shown in Figure 7c. Only 65% dyes were decomposed after 3 h, and this is lower than P25. This can be attributed to the small surface area. Though the total BET surface area is determined to be 6.8 m^2/g, the effective outside surface for photocatalysis is even smaller, leading to the lower efficiency.

On the basis of the above evolution information and comparison with other literature results, we propose the whole formation process of the mosaic spheres is dominated by two growth modes, the aggregation tendency of anatase crystals and simultaneous development of reactive facets mediated by fluorine anions. As the reaction was conducted at high temperature in the absence of long-chain surfactants, Ti^{3+} ions could easily nucleate and grow up via hydrolysis reaction, forming aggregated particles of loose structure because of the relatively small sizes of the building blocks. These blocks are also covered with reactive planes rather than irregular particles, owing to regulation of F ions on the surface. With the growing up of surface units via the Ostwald ripening process, the whole surface of the micrometer spheres will gradually be completely covered by anatase (001) facets, forming mosaic structures. In brief, it is the cooperative behavior of aggregation and inducing effects of F ions on anatase (001) facets that promote formation of such mosaic spheres.

CONCLUSION

In summary, pseudo-isotropic mosaic spheres almost completely covered with reactive anatase {001} facets have been prepared via a one-pot reaction in the presence of NaF serving as both morphology-controlling agent and phase chooser. This kind of structure has an apparent isotropic effect owing to the quite large exposure fraction of reactive facets, such as the corresponding XRD diffractive intensity of the (004) facet which has been promoted by nearly 2 orders of magnitude. The current results would offer an ideal research platform for the fundamental issues related with surface chemistry and physics, reactive facets involved crystal plane effects, catalysis, etc.

ASSOCIATED CONTENT

Supporting Information. More information of SEM and XRD results showing the evolution of (004) peak intensities. This material is available free of charge via the Internet at http://pubs.acs.org.

dx.doi.org/10.1021/ic200553t |*Inorg. Chem.* 2011, 50, 6237–6242

AUTHOR INFORMATION

Corresponding Author
*Phone: 86-10-62792791. E-mail: wangxun@mail.tsinghua.edu.cn.

ACKNOWLEDGMENT

This work was supported by the NSFC (Grant 20725102, 20921001) and the State Key Project of Fundamental Research for Nanoscience and Nanotechnology (Grant 2011CB932402).

REFERENCES

(1) Li, S. C.; Chu, L. N.; Gong, X. Q.; Diebold, U. *Science* **2010**, *328*, 882.
(2) Wendt, S.; Sprunger, P. T.; Lira, E.; Madsen, G. K. H.; Li, Z. S.; Hansen, J. O.; Matthiesen, J.; Blekinge-Rasmussen, A.; Laegsgaard, E.; Hammer, B.; Besenbacher, F. *Science* **2008**, *320*, 1755.
(3) Matthey, D.; Wang, J. G.; Wendt, S.; Matthiesen, J.; Schaub, R.; Laegsgaard, E.; Hammer, B.; Besenbacher, F. *Science* **2007**, *315*, 1692.
(4) Schaub, R.; Wahlstrom, E.; Ronnau, A.; Laegsgaard, E.; Stensgaard, I.; Besenbacher, F. *Science* **2003**, *299*, 377.
(5) Tian, N.; Zhou, Z. Y.; Sun, S. G.; Ding, Y.; Wang, Z. L. *Science* **2007**, *316*, 732.
(6) Zhang, D. Q.; Li, G. S.; Yang, X. F.; Yu, J. C. *Chem. Commun.* **2009**, *45*, 4381.
(7) Yang, H. G.; Sun, C. H.; Qiao, S. Z.; Zou, J.; Liu, G.; Smith, S. C.; Cheng, H. M.; Lu, G. Q. *Nature* **2008**, *453*, 638.
(8) Han, X. G.; Kuang, Q.; Jin, M. S.; Xie, Z. X.; Zheng, L. S. *J. Am. Chem. Soc.* **2009**, *131*, 3152.
(9) Yang, H. G.; Liu, G.; Qiao, S. Z.; Sun, C. H.; Jin, Y. G.; Smith, S. C.; Zou, J.; Cheng, H. M.; Lu, G. Q. *J. Am. Chem. Soc.* **2009**, *131*, 4078.
(10) Zheng, Z. K.; Huang, B. B.; Qin, X. Y.; Zhang, X. Y.; Dai, Y.; Jiang, M. H.; Wang, P.; Whangbo, M. H. *Chem.—Eur. J.* **2009**, *15*, 12576.
(11) Liu, M.; Piao, L. Y.; Zhao, L.; Ju, S. T.; Yan, Z. J.; He, T.; Zhou, C. L.; Wang, W. J. *Chem. Commun.* **2010**, *46*, 1664.
(12) Sun, Y. G.; Xia, Y. N. *Science* **2002**, *298*, 2176.
(13) Xiang, G. L.; Zhuang, J.; Wang, X. *Inorg. Chem.* **2009**, *48*, 10222.
(14) Xiang, G. L.; Li, T. Y.; Zhuang, J.; Wang, X. *Chem. Commun.* **2010**, *46*, 6801.
(15) Li, H. X.; Bian, Z. F.; Zhu, J.; Zhang, D. Q.; Li, G. S.; Huo, Y. N.; Li, H.; Lu, Y. F. *J. Am. Chem. Soc.* **2007**, *129*, 8406.
(16) Jiang, X. C.; Herricks, T.; Xia, Y. N. *Adv. Mater.* **2003**, *15*, 1205.
(17) Read, C. G.; Steinmiller, E. M. P.; Choi, K. S. *J. Am. Chem. Soc.* **2009**, *131*, 12040.
(18) Hu, L. H.; Peng, Q.; Li, Y. D. *J. Am. Chem. Soc.* **2008**, *130*, 16136.
(19) Liu, G.; Yang, H. G.; Wang, X. W.; Cheng, L. N.; Pan, J.; Lu, G. Q.; Cheng, H. M. *J. Am. Chem. Soc.* **2009**, *131*, 12868.
(20) Pan, J. H.; Zhang, X. W.; Du, A. J.; Sun, D. D.; Leckie, J. O. *J. Am. Chem. Soc.* **2008**, *130*, 11256.